Journal of Thermal Analysis and Calorimetry (2023) 148:6423–6437
https://doi.org/10.1007/s10973-023-12159-4

CO_2 gasification behavior of chars from high-alkali fuels and effects of Na, K, Ca, and Fe species via synthetic coal char

Lin Zhao[1] · Chang'an Wang[1] · Maoyun Luo[1] · Pengbo Zhao[1,2] · Defu Che[1]

Received: 18 November 2022 / Accepted: 25 March 2023 / Published online: 15 April 2023

Abstract
The study on CO_2 gasification behavior helps to promote the clean and efficient utilization of high-alkali fuels. The high-alkali fuels feature high contents of alkali metals, and sometimes they are also rich in alkali earth metals and iron. Though the influences of minerals on gasification characteristics have been extensively studied, few researchers have selected minerals based on the ash composition of high-alkali fuel. Moreover, the complex interactions among minerals could lead to inaccurate conclusions. In this paper, the CO_2 gasification behavior of chars originated from one high-alkali biomass and three high-alkali coals was studied. The effects of principal minerals related to the high-alkali fuels, which were determined through the new plasma ashing method and traditional muffle ashing method, were also further evaluated via synthetic coal char. The synthetic coal char was free from any intrinsic minerals. The results indicate that the gasification reactivities of chars from high-alkali fuels are positively associated with the reaction temperature (900–1200 °C). The biomass char possesses the highest gasification reactivity, and three coal char samples are inferior to various degrees. The related chemicals offer their catalytic activities at 1000 °C in the sequence of K/Na-containing chemicals > Fe-containing chemicals > Ca-containing chemicals. The shrinking core model (SCM) and two-dimensional growth of nuclei model (2DGM) were chosen to conduct the kinetic analysis. The reaction constants of chars from different high-alkali fuels agree with their gasification behavior. Generally, the 2DGM is more suitable than SCM to predict the conversion of selected char samples. In most cases, the additions of chemicals increase the reaction constants. When Fe_2O_3 and $CaCO_3$ are added into synthetic coal char, the SCM is more accurate to describe the gasification behavior at 900 °C, but the addition of Na_2SO_4 makes the 2DGM a better one.

Keywords High-alkali fuel · CO_2 gasification · Plasma ashing method · Synthetic coal · Kinetic analysis

Introduction

The high-alkali fuels, such as biomass and high-alkali coal, are playing an important part in the global energy consumption. Among them, biomass is regarded as a promising alternative to fossil fuel because of its renewability, CO_2-neutrality, and wide distribution [1, 2]. Meanwhile, the high-alkali coal, like Zhundong coal, is expected to meet the ever-growing energy demand due to its huge reserve [3]. Hence, the clean and efficient utilization of high-alkali fuel is of great significance for the global energy supply and environmental protection.

Gasification and oxy-fuel combustion have been regarded as promising ways to utilize high-alkali fuel because they are conducive to the reductions of carbon emission and air pollutant emission [4–6]. The CO_2 gasification are important in both processes. In the gasifier, solid fuel reacts with gasifying agent (usually one or a mixture of oxygen, air, and steam) to produce the syngas, which is convenient to store and transport. Many reactions take place during the gasification process, and the reaction between CO_2 and char is one of the most important ones [7]. Furthermore, the flue gas from the oxy-fuel combustion, which mainly consists of CO_2 and H_2O, has been proposed as a new gasifying agent to reduce CO_2 emission [8]. In that case, the reaction between CO_2 and char is likely to be more important than it is when the traditional gasifying agent is employed. It is worth noting that the CO_2 gasification appears not only in the gasifier,

✉ Chang'an Wang
changanwang@mail.xjtu.edu.cn

[1] State Key Laboratory of Multiphase Flow in Power Engineering, School of Energy and Power Engineering, Xi'an Jiaotong University, Xi'an 710049, China

[2] Xi'an TPRI Boiler and Environmental Protection Engineering Co., Ltd., Xi'an 710054, China

but also in the boiler if the air-staged combustion technology, which is an effective method to reduce nitrogen oxide emission, is applied [9]. The CO_2 gasification occurs when the deficient oxygen is consumed in the main combustion zone and the over fired air is not injected into the furnace yet. If the oxygen-staged oxy-fuel combustion technology is applied, the CO_2 gasification is supposed to be triggered more easily owing to the high CO_2 content. Therefore, the deep knowledge about CO_2 gasification behavior is crucial to promote the clean and efficient utilization of high-alkali fuel.

It is generally reported that the CO_2 gasification behavior of char could be influenced by some chemicals containing alkali metals (e.g., Na_2CO_3, K_2CO_3, $NaAlO_2$) [10, 11], alkali earth metals (e.g., $Ca(NO_3)_2$, $CaCO_3$) [12, 13], and transition metals (e.g., $FeCO_3$, $NiNO_3{\cdot}6H_2O$) [14, 15]. The high-alkali fuels feature high contents of alkali metals, and sometimes they are also rich in alkali earth metals and iron [16]. As a result, the minerals in high-alkali fuels are likely to have a significant effect on the CO_2 gasification. However, many minerals investigated in the previous studies are absent in raw high-alkali fuels or during the transformation process of high-alkali fuels. For instance, Na_2CO_3 has been extensively studied as an efficient catalyst for CO_2 gasification [10, 11, 17, 18], while the Na-containing chemicals are mostly NaCl and Na_2SO_4 rather than Na_2CO_3 in raw high-alkali fuels, and Na tends to exist in the forms of silicate and aluminosilicate at high temperature, if not volatilized [19]. Undeniably, some minerals related to high-alkali fuels were investigated, but the species were limited because the researchers paid attention to other fuels instead of high-alkali fuels [10, 12, 20]. Therefore, it is necessary to focus on the high-alkali fuels and study the effects of related minerals (Na, K, Ca, and Fe species), which helps to better understand the gasification characteristic of high-alkali fuel char and find proper catalysts as well.

In order to determine the main minerals that exist in raw high-alkali fuels and during the transformation process of high-alkali fuels, ash samples need to be prepared for characterization. However, the traditional ashing method using a muffle furnace is probably inappropriate to identify the minerals in raw fuel due to the mineral formation and transformation at high temperature [21]. In recent years, the plasma ashing method has been considered as an effective way to avoid this problem [19, 22]. The new method is able to consume organic matter at low temperature (< 200 °C) so the mineral species can remain in the original state, which gives accurate information of minerals in raw fuel. The minerals that exist during the transformation process of high-alkali fuels can be identified in the ash samples prepared by the traditional ashing method.

After the minerals related to the high-alkali fuels are selected, the carrier needs to be determined. In the previous studies on the effects of minerals, the additive chemicals were usually loaded on raw fuel or char [10, 12, 13]. The intrinsic minerals in raw fuel and char probably react with the additive chemicals during the CO_2 gasification, so it is difficult to specifically study the effects of additive chemicals. Even though the experimental subjects were demineralized by HCl and HF in some previous research [11, 17], the residual halogen in acid-treated subjects still may affect the additive chemicals. Unlike the natural or acid-treated experimental subjects, the synthetic coal is free from any intrinsic minerals, so the complex interaction among minerals can be avoided [23, 24]. The combustion characteristics of synthetic coal have already been demonstrated to be similar to those of real coal, which means the synthetic coal is qualified to simulate the real coal in terms of combustion performance [23, 24]. If the synthetic coal and real high-alkali fuels have similar CO_2 gasification behavior, it can be employed to accurately study the effects of minerals related to high-alkali fuels on CO_2 gasification.

In the present study, the char samples of different high-alkali fuels were prepared at first to study their gasification behavior. Afterwards, the new plasma ashing method and traditional muffle ashing method were applied to determine the main minerals that existed in raw high-alkali fuels and during the transformation process of high-alkali fuels. The synthetic coal char without any intrinsic minerals was employed to carry the minerals related to high-alkali fuels to investigate their impacts on gasification. Finally, two kinetic models, shrinking core model and two-dimensional growth of nuclei model, were selected to conduct the kinetic analysis. The present study on the gasification reactivities of high-alkali fuels and on the kinetic analysis is expected to provide useful information about the design of gasifier and optimization of reaction condition. The work about the catalytic influence of mineral helps to find proper catalysts, which could reduce the energy consumption and make the reaction condition milder.

Experimental

Raw samples

One high-alkali biomass, wheat straw (abbreviated as WS, hereinafter), three high-alkali coals, Lu'an (LA) coal, Zijin (ZJ) coal, and Tianchi (TC) coal, were chosen to study the gasification characteristics of high-alkali fuels in the present research. Besides these common high-alkali fuels, one synthetic coal (SC) was also prepared to evaluate the effects of some minerals related to the high-alkali fuels on gasification. The synthetic coal in this study contains no minerals, therefore complex interactions between intrinsic minerals in raw fuels and additive chemicals can be avoided. The preparation of synthetic coal was described briefly as follows: firstly,

the raw material of synthetic coal was obtained by mixing cellulose and 8-hudroxyquinoline in a mass ratio of 4:1; secondly, the mixture was put into an autoclave where the temperature and pressure were 200 °C and 20 MPa, respectively, and the conditions were maintained for 24 h; thirdly, the product was collected from the autoclave, which served as the synthetic coal in the subsequent experiments. More detailed information about the preparation of synthetic coal can be found in our previous studies [23, 24]. These four high-alkali fuels and synthetic coal were crushed and sieved into particles < 100 μm for the subsequent pyrolysis experiments. Their proximate and ultimate analyses on air-dried basis are listed in Table 1.

In order to determine the main minerals that exist in raw high-alkali fuels and during the transformation process of high-alkali fuels, two different methods (plasma ashing method and traditional ashing method) were applied to prepare the ash samples. A plasma oxidation device (K1050X) from Emitech was employed to prepare the low-temperature plasma ash (LTA) samples with the operating temperature < 200 °C. The plasma ashing method is capable of consuming organic matter without destroying the initial state of mineral, which gives the information of original minerals in raw high-alkali fuels [19, 22]. The traditional ashing method was carried out to prepare the high-temperature ash (HTA) samples at 815 °C by a muffle furnace according to Chinese standard GB/T 1574-2007, which could give the information of minerals during the transformation process of high-alkali fuels. The X-ray fluorescence (XRF) analysis was conducted using an S4 PIONEER from Bruker AXS to measure the chemical compositions of different ash samples. The XRF results are listed in Table 2 (LTA samples) and Table 3 (HTA samples). The LTA and HTA samples have different compositions because the high temperature in traditional ashing method can lead to the volatilization, decomposition, and other reactions of minerals in raw fuel. Generally, the raw high-alkali fuel contains more minerals than the traditional ashing method shows. More information about the effects of ashing method and temperature on the ash composition can be accessed in our previous study [19]. Based on the ash compositions, K-containing chemical (KCl), Na-containing chemicals (NaCl, Na_2SO_4, Na_2SiO_3), Ca-containing chemicals ($CaCO_3$, $CaSO_4$), and Fe-containing chemicals (Fe_2O_3, Fe_3O_4) were selected to study their influences on gasification behavior. This part of research could also help to study the feasibility of using high-alkali fuel ash as catalyst for gasification. The high-alkali fuel ash is potential to serve as effective catalysts with broad resource and low cost.

Table 1 Proximate and ultimate analyses of high-alkali fuels (air-dried basis)

Samples	Proximate analysis/%				Ultimate analysis/%				
	w(FC)	*w* (V)	*w* (A)	*w* (M)	*w* (C)	*w* (H)	*w* (O)[a]	*w* (N)	*w* (S)
WS	47.65	36.17	7.58	8.60	40.12	4.81	38.29	0.47	0.13
LA	50.47	31.78	10.92	6.83	61.35	2.97	17.22	0.57	0.14
ZJ	53.76	28.42	3.52	14.30	64.77	3.72	12.34	0.77	0.58
TC	65.10	25.96	4.06	4.88	73.50	2.79	14.08	0.13	0.56
SC	68.88	31.09	0.00	0.03	65.37	2.86	28.29	3.45	0.00

[a] $w(O) = 100 - w(C) - w(H) - w(N) - w(S) - w(A) - w(M)$

Table 2 Compositions of low-temperature plasma ash samples (mass%)

Samples	*w* (SiO_2)	*w* (Al_2O_3)	*w* (TiO_2)	*w* (Fe_2O_3)	*w* (CaO)	*w* (MgO)	*w* (K_2O)	*w* (Na_2O)	*w* (SO_3)	*w* (Cl)
WS	46.3	0.9	0.1	1.1	5.2	1.25	21.8	0	3.3	17.5
LA	17.2	9.4	0.8	7.3	38.3	2.4	0.6	5.5	3.8	13.6
ZJ	11.2	9.6	0.53	13.9	18.7	1.4	0.07	9.7	16.2	18.0
TC	4.9	5.3	0.3	3.8	37.3	4.5	0.2	6.2	30.1	6.2

Table 3 Compositions of high-temperature ash samples (mass%)

Samples	*w* (SiO_2)	*w* (Al_2O_3)	*w* (TiO_2)	*w* (Fe_2O_3)	*w* (CaO)	*w* (MgO)	*w* (K_2O)	*w* (Na_2O)	*w* (SO_3)	*w* (Cl)
WS	62.8	1.1	0.1	1.4	6.2	1.4	18.0	0	4.5	1.4
LA	23.2	13.1	0.9	9.1	40.0	3.6	0.2	3.3	3.2	2.7
ZJ	17.2	17.1	0.64	19.3	20.1	3.3	1.07	8.9	10.9	0.25
TC	6.6	6.8	0.4	9.5	44.8	6.0	0.1	1.3	20.1	1.5

Char preparation

The char samples of four high-alkali fuels and synthetic coal were prepared in an electrically-heated tube furnace. During each pyrolysis experiment, about 1.5 g raw sample in an alumina crucible was placed into the reaction zone of the tube furnace under the nitrogen atmosphere (1 L min^{-1}). The raw sample was subjected to a heating rate of 10 °C min^{-1} up to 1200 °C and maintained at the pre-set temperature for 60 min. The gasification temperature of solid fuel is selected based on its property, usually in the range from 900 to 1600 °C [25]. Therefore, an intermediate temperature, i.e. 1200 °C, was chosen to prepare char samples for gasification experiment in this study. After the product was cooled to ambient temperature in the nitrogen stream, it was collected for the following experiments, including the scanning electron microscopy (SEM) analysis coupled with energy dispersive spectroscopy (EDS) analysis, and gasification experiment. The SEM–EDS analysis was performed by a Tecnai G2-F30 to investigate the morphology and element distribution of char samples originated from four high-alkali fuels and synthetic coal. The char samples of four high-alkali fuels were directly used for the subsequent gasification experiments, while the char samples of synthetic coal were mixed mechanically with additive chemicals in a mass ratio of 9:1 to evaluate the effects of minerals related to high-alkali fuels on gasification. In the respect of catalysts, the present work mainly focused on the species of mineral, and the influence of additive content might be studied in the future work.

Gasification experiment

Thermal analyzer has been widely adopted to study the conversion of solid fuel [26–30]. The gasification experiments were conducted using a Setaram simultaneous thermal analyzer Labsys Evo. The buoyancy and temperature calibrations were conducted before the gasification experiments, and the standard error for temperature reading was 1.5 °C. For each experiment, 20 ± 0.2 mg of experimental sample was loaded into an alumina crucible and heated from ambient temperature to the pre-set temperature (900 °C, 1000 °C, 1100 °C, 1200 °C) at a rate of 20 °C min^{-1} under the nitrogen atmosphere (10 mL min^{-1}). Once the pre-set temperature was reached, the temperature remained unchanged and the atmosphere was switched to N_2 (10 mL min^{-1}) and CO_2 (40 mL min^{-1}) to trigger the isothermal gasification. Usually, 60 min was long enough to finish the isothermal gasification, while it took longer at low reaction temperature. Prior to each group of formal experiments, the blank experiment was conducted at least twice. Some formal gasification experiments were also repeated to verify the accuracies of experimental results, which indicated a good repeatability. In addition, the reliability of thermal analyzer used in this study was also demonstrated in our previous research [31].

The carbon conversion ratio (x) was calculated by the following equation [32–34]:

$$x = \frac{w_0 - w_t}{w_0 - w_{ash}} \tag{1}$$

where w_0 represents the initial mass of sample, w_{ash} denotes the mass of residual ash after complete gasification, and w_t is the instantaneous mass of sample at time of t.

The reactivity index $R_{0.5}$ was defined to quantify the char gasification reactivity as follows [17, 35]:

$$R_{0.5} = \frac{0.5}{\tau_{0.5}} \tag{2}$$

where $\tau_{0.5}$ is the time (min) that it takes for x to reach 0.5.

Kinetic analysis

Many kinetic models have been applied by researchers to conduct the kinetic analysis of char gasification [36–38]. A universal method to select appropriate models is comparing many models to experimental data [36–38], which is time-consuming. Some researchers [39] proposed that appropriate models could be determined by fitting the experimental data according to the Avrami and Erofe'ev equations. The equations are shown as follows [33, 39–41]:

$$x = 1 - \exp(-kt^m) \tag{3}$$

$$\ln(-\ln(1-x)) = \ln k + m \ln t \tag{4}$$

where k represents the reaction constant dependent on nucleation frequency and grain growth rate, m denotes the constant associated with the geometry of the reaction system. According to Eq. (4), the curve $\ln(-\ln(1-x))$ versus $\ln t$ is expected to be linear, the slope m of which indicates the multiple reaction pathways and the most possible mechanisms. Therefore, appropriate kinetic models can be selected based on m to determine the reaction constant k in different cases. Usually, the conversion ratio (x) was limited to 0.15–0.50 to obtain m because the acceleratory region (x = 0.15–0.50) was considered to be qualified for exploring reaction mechanisms [39, 42, 43]. Mathematically the Avrami and Erofe'ev equation represents a sigmoid $x \sim t$ curve, while the experimental data is fitted in a certain x range, i.e. x = 0.15–0.50. Hence, this method does not require that the whole experimental curve is sigmoid, and the selected models might not be sigmoid, either.

The *mean absolute percentage error* (*MAPE*) was employed to measure the deviation between the experiment data and calculated data obtained based on selected kinetic model [44]:

$$\mathrm{MAPE} = \frac{100\%}{n}\sum_{i=1}^{n}\left|\frac{\hat{x}_i - x}{\hat{x}_i}\right| \quad (5)$$

where $\hat{x}_i$ and x_i represent the carbon conversion ratios from experiment data and from calculated data at the same reaction time, respectively. In this research, $\hat{x}_i$ was in the range of 0.1–0.9 with the interval of 0.1, which meant $n = 9$.

Results and discussion

Gasification behavior of chars from different high-alkali fuels

The carbon conversion ratios (x) of char samples originated from different high-alkali fuels as a function of time (t), are presented in Fig. 1, and the corresponding gasification reactivity indexes ($R_{0.5}$) are shown in Fig. 2. According to the $x \sim t$ curves and $R_{0.5}$, the gasification reactivities of char

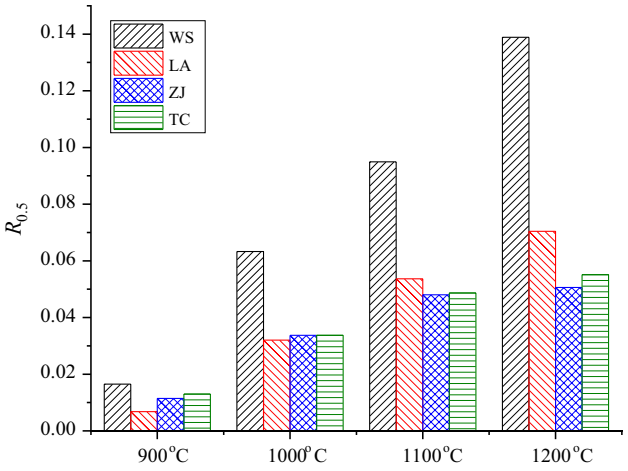

Fig. 2 $R_{0.5}$ of different high-alkali chars

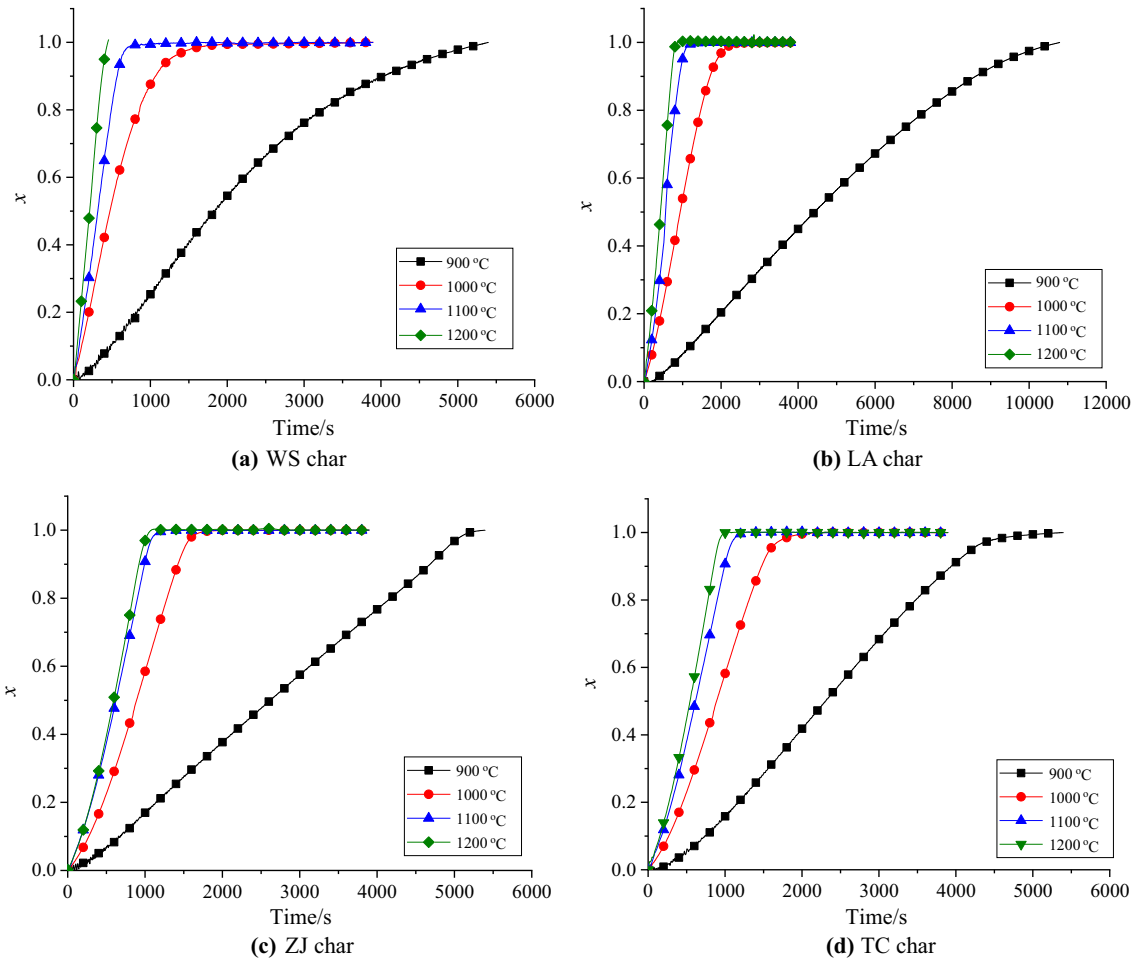

Fig. 1 Carbon conversion ratio (x) versus time (t) curves for different high-alkali chars

samples depend heavily on reaction temperature and the variation tendencies with temperature are similar. At 900 °C, it takes longer than 5000 s for these char samples to finish the isothermal gasification, especially for LA char, which requires about 11,000 s. The reaction time at 1000 °C is less than 2000s for all four char samples, indicating their gasification reactivities are significantly enhanced due to the increased temperature. The reaction time is further reduced when the temperature rises from 1000 to 1100 °C, at which 1000 s is long enough for gasifying agent to convert carbon completely. However, it is hardly achievable to promote char gasification by increasing reaction temperature at > 1100 °C because the $x \sim t$ curves at 1200 °C are relatively close to those at 1100 °C. It is still feasible to promote char gasification by increasing reaction temperature at > 1100 °C. However, the promoting effects are moderated, given the fact that the $x \sim t$ curves at 1200 °C are close to those at 1100 °C. The enhancement caused by increasing temperature is due to the endothermic nature of gasification [45]. The raw fuel determines the char characteristics, including the texture structure, functional group, mineral, and so on, therefore the category of raw high-alkali fuel also substantively affects the gasification reactivity of char [46, 47]. As shown in Figs. 1 and 2, WS char possesses the highest gasification reactivity at 900–1200 °C, and three coal char samples are inferior to various degrees. The char samples from two Zhundong coals, ZJ char and TC char, have broadly similar $x \sim t$ curves and $R_{0.5}$. The LA char has lower gasification reactivity than ZJ and TC chars at 900 °C and 1000 °C, while it is more reactive at 1100 °C and 1200 °C. According to Table 2, the total content of CaO, SiO_2, and Al_2O_3, in the LTA of LA coal is up to 64.9%, implying that calcium aluminosilicates are the main minerals in LA coal. Perhaps these minerals have low catalytic activities at low temperature, while they can promote the gasification significantly at high temperature. Moreover, the structure and functional group of LA char are also probably related to the gasification behavior, which might be investigated in the future study.

The char samples of different high-alkali fuels were subjected to SEM–EDS analysis for the knowledge of micromorphology and elemental distribution, and the results are shown in Fig. 3. As demonstrated in SEM images, plenty of long fibrous particles with stacked structure are observed in WS char, while these three coal char samples are mainly composed of irregular block-shaped particles of varying sizes. It seems that the stacked structure is partly responsible for the high reactivity of WS char because the structure leads to large area for gasification. In the enlarged images, it can be seen that there are lots of teeny-tiny particles attached to the surfaces of large ones. The comparison between the LTA and HTA implies that high temperature leads to the volatilization and decomposition of some minerals. Similar changes is likely to occur in the preparation of char samples, so it is possible that some small particles originate from broken mineral matter. The char samples were subjected to EDS analysis to study the element distribution of particle surface that covers tiny particles. For WS char, the inorganic elements like Si and Ca account for a considerable proportion of chosen area, implying some tiny particles mainly consist of minerals rather than carbon. For the three coal char samples, however, the chosen areas show extremely low content of inorganic elements, indicating the organic matters dominate the tiny particles. Many minerals like AAEMs have been reported to be able to serve as effective catalysts for gasification [13, 17, 35]. Therefore, the widespread minerals on the surfaces of WS char are supposed to be one of reasons that WS char possess higher gasification reactivity than other three coal char samples.

Effects of minerals related to high-alkali fuels on gasification

The synthetic coal with a known composition was prepared to represent the gasification behavior of real coal. Given the char derived from synthetic coal is free of mineral matter, complex interactions among minerals can be avoided when the impacts of some certain minerals on gasification are investigated. The similarity in combustion behavior between synthetic coal and real coal has already been reported in our previous studies [23, 24]. The gasification behavior and micro-morphology of SC char are displayed in Fig. 4. For $x \sim t$ curves of SC char, the variation tendency with temperature is similar to those of WS, LA, ZJ, and TC chars. The reaction time and $R_{0.5}$ are also close to those of the four char samples, at least they are in the same order of magnitude. Furthermore, the particles in SC char are mostly irregular block-shaped particles of varying sizes, which agrees with the char samples originated from the three high-alkali coal. Hence, the SC char is believed to be qualified for subsequent investigations on the effects of minerals related to high-alkali fuels on gasification.

The alkali metals in high-alkali fuels are inclined to volatilize during the heating process, corresponding to the lower alkali metal contents in high-temperature ash samples. As listed in Tables 2 and 3, the high-temperature ash samples have substantially less chlorine than the plasma ash samples, and for high-alkali coals, the SO_3 contents in the high-temperature ash samples are also lower than those in the plasma ash samples. It implies that some alkali metals in raw high-alkali fuels volatilize in the forms of chloride

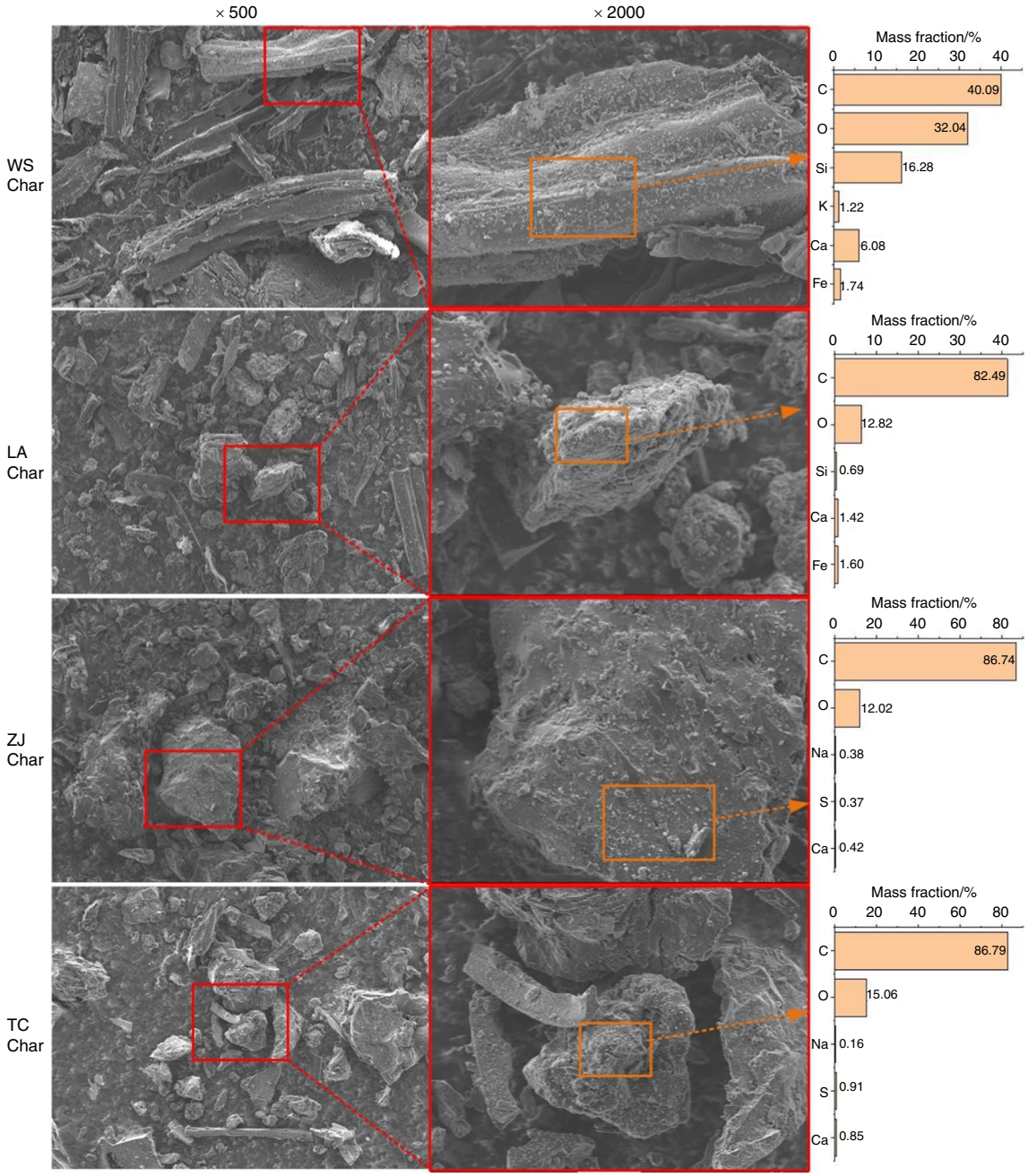

Fig. 3 SEM images and EDS analysis results of different high-alkali chars

and sulfate during the heating process, and the rest of them transform into more stable minerals like silicates and aluminosilicates [19]. Considering the raw minerals and transformed minerals, different alkali metal compounds (KCl, NaCl, Na_2SO_4, Na_2SiO_3) were selected to evaluate the effects of typical minerals on gasification. In addition, the ash samples of high-alkali coals have high contents of CaO and Fe_2O_3 according to the XRF results. Therefore, Ca-containing chemicals ($CaCO_3$, $CaSO_4$) and Fe-containing chemicals (Fe_2O_3, Fe_3O_4) were also selected in the present study. More information about the minerals in high-alkali fuels can be found in our previous studies [16, 19].

The gasification behavior of SC char catalyzed by the chemicals at 1000 °C is depicted in Fig. 5, which show that

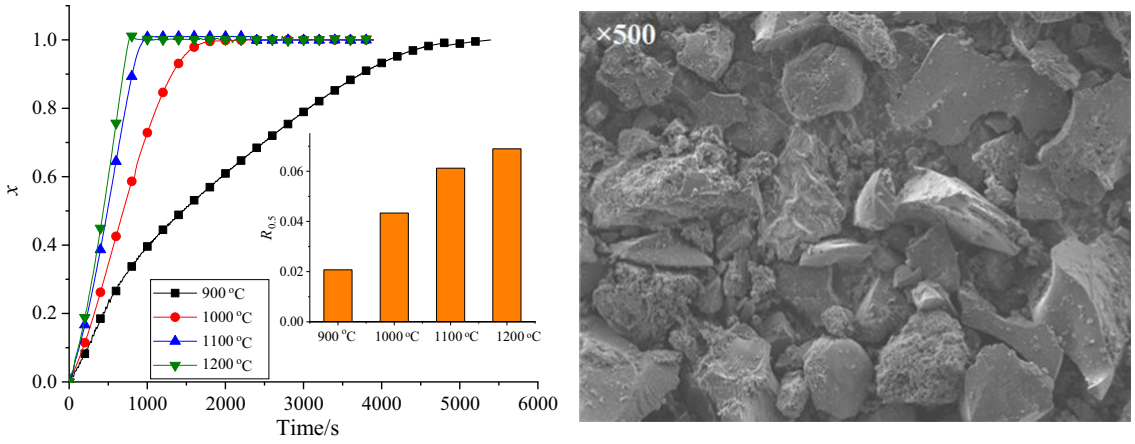

(a) Gasification behavior **(b)** Micro-morphology

Fig. 4 Gasification behavior and micro-morphology of SC char

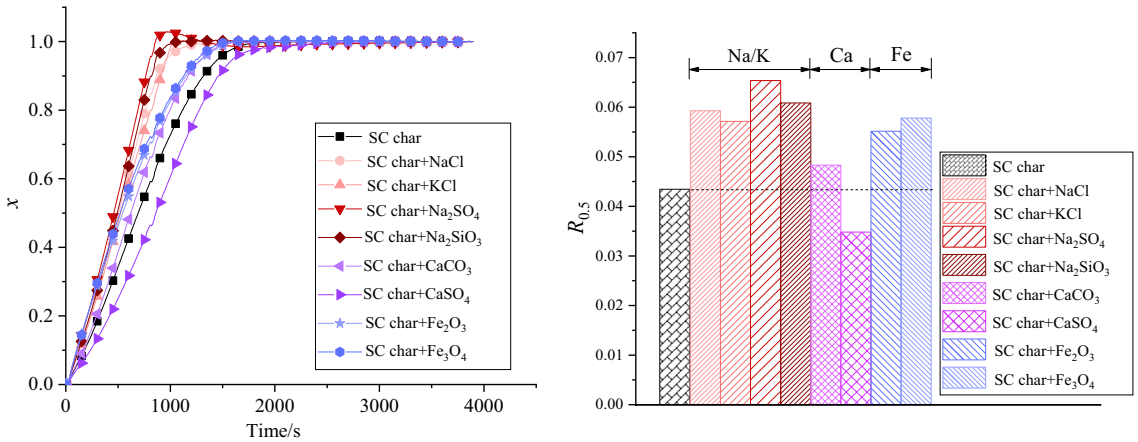

(a) *x-t* curves (b) gasification reactivity indexes

Fig. 5 Effects of Na, K, Ca, and Fe species on gasification at 1000 °C via SC char

most chosen chemicals can enhance the char gasification to various degrees. According to the *x-t* curves and $R_{0.5}$, the promoting impact of NaCl is similar to that of KCl, and Na_2SO_4 has a better catalytic performance than both of them. Since Na_2SO_4 can react with char carbon to produce Na_2S, there are more newly generated pores in SC char, leading to larger surface area and more active sites for gasification [17, 48]. Furthermore, the oxygen-containing functional groups on char surface from the reaction between char and minerals can weaken the adjacent carbon–carbon bonds, making them susceptible to the attack from the oxidant [35]. Theoretically Na_2SO_4 has the ability to supply oxygen when the oxygen-containing functional groups are formed because Na_2SO_4 contains oxygen atoms, while NaCl and KCl have to react with oxygen atoms in SC char. Hence, Na_2SO_4 is more efficient to improve gasification reactivity of SC char than NaCl and KCl. As a common Na-containing chemicals present in high-alkali fuel ash, Na_2SiO_3 has an obvious promoting influence on gasification, which means it is potential for high-alkali fuel ash to serve as effective catalysts with broad resource and low cost. It is observed that the Fe-containing chemicals (Fe_2O_3, Fe_3O_4) are also beneficial to char gasification. It is worthy to note that Fe_2O_3 and Fe_3O_4 are often identified in ash samples of some high-alkali fuels [19], so they can play a facilitating role in char gasification once high-alkali fuel ash is employed as catalysts. As for Ca-containing chemicals, the presence of $CaCO_3$ slightly increases the reaction rate according to the *x*−*t* curves and $R_{0.5}$, while $CaSO_4$ exerts a negative influence on char gasification. Li et al. [49] pointed out that it was CaO, rather than $CaCO_3$ or $CaSO_4$, that had catalytic ability. In this study, the isothermal gasification was conducted at 1000 °C, which was high enough for $CaCO_3$ to decompose into CaO, but not high enough for $CaSO_4$ because pure $CaSO_4$ could not

decompose below 1200 °C [50]. Moreover, $CaSO_4$ is supposed to cover some char surfaces, keeping them away from CO_2. Consequently, the presence of $CaSO_4$ delays the carbon conversion. Although some chemicals like Fe_2O_3 and $CaCO_3$, are not as efficient as alkali salts, they still can promote the gasification. Therefore, the low-alkali coal is also likely to possess high gasification reactivity if it has high contents of these minerals. Generally, the selected chemicals offer their catalytic activities at 1000 °C in the sequence of K/Na-containing chemicals > Fe-containing chemicals > Ca-containing chemicals.

Kinetic analysis of gasification of chars from different high-alkali fuels

The fitting parameters listed in Table 4 were calculated in the range of $x = 0.15$–0.50 according to Eq. (3) and (4). It can be seen that all values of m are between 1 and 2 with the squares of correlation coefficients (R^2) higher than 0.99. Table 5 lists some common kinetic models for gas–solid reaction with different m [33, 39]. Since the values of m in Table 4 fluctuate and there is no model that perfectly matches them, the models with $m = 1$–2 are possibly proper for the high-alkali char gasification. Hence, the phase boundary controlled model (contracting sphere), which is also named as the shrinking core model (SCM, $m = 1.07$), and the two-dimensional growth of nuclei model (2DGM, $m = 2$) were selected in the present study.

According to the equations of SCM and 2DGM in Table 5, the reaction constants (k) of high-alkali chars can be determined by linear regression analysis. Taking the gasification of WS char as an example, Fig. 6 displays the application of SCM and 2DGM to the experimental results. The slope of each fitting linear is the reaction constant for each reaction temperature. The reaction constants of other high-alkali chars were also obtained using the same method, and the results are listed in Table 6. The R^2 in linear regression analysis are all higher than 0.98, indicating significant linear correlations. As listed, the reaction constants of high-alkali chars obviously increase when the reaction temperature gets higher, and WS char has a higher reaction constant than other high-alkali chars at the same reaction temperature. The influences of reaction temperature and char category on the reaction constant determined based on both the SCM and 2DGM agree with the gasification behavior shown in Figs. 1 and 2. In addition, the application of 2DGM can lead to a slightly higher reaction constant than the SCM under the same condition.

In order to verify the accuracies of selected kinetic models in describing the gasification behavior of high-alkali chars, the calculated $x \sim t$ curves based on the SCM and 2DGM are compared with the experiment data in Fig. 7. The calculated curves were obtained according to the equations in Table 5 and the reaction constants in Table 6, and the deviations between the experiment data and calculated data were measured quantitatively using the *mean absolute percentage error* (*MAPE*) according to Eq. (5). It can be seen that the SCM is more suitable to predict the gasification behavior of WS char at 900 °C and 1000 °C, while the 2DGM fits better at 1100 °C and 1200 °C. The SCM assumes that the reaction takes place at the outside surface of char particle and moves inward once

Table 4 Fitting parameters of high-alkali chars in the range of $x = 0.15$–0.50

Temperature/°C	WS char		LA char		ZJ char		TC char	
	m	R^2	m	R^2	m	R^2	m	R^2
900	1.40	0.9994	1.39	0.9999	1.36	0.9998	1.65	0.9970
1000	1.29	0.9993	1.46	0.9991	1.65	0.9984	1.61	0.9991
1100	1.30	0.9977	1.63	0.9904	1.54	0.9977	1.57	0.9971
1200	1.27	0.9958	1.40	0.9971	1.59	0.9962	1.55	0.9969

Table 5 Some kinetic models for gas–solid reaction

Kinetic model	Equation	m
One-dimensional diffusion	$x^2 = kt$	0.62
Two-dimensional diffusion	$(1-x)\ln(1-x) + x = kt$	0.57
Three-dimensional diffusion	$[1-(1-x)^{1/3}]^2 = kt$	0.54
First order reaction (also named as volumetric model)	$-\ln(1-x) = kt$	1
Phase boundary controlled (contracting sphere, also named as shrinking core model)	$3[1-(1-x)^{1/3}] = kt$	1.07
Phase boundary controlled (contracting cylinder)	$1-(1-x)^{1/2} = kt$	1.11
Two-dimensional growth of nuclei	$[-\ln(1-x)]^{1/2} = kt$	2
Three-dimensional growth of nuclei	$[-\ln(1-x)]^{2/3} = kt$	3

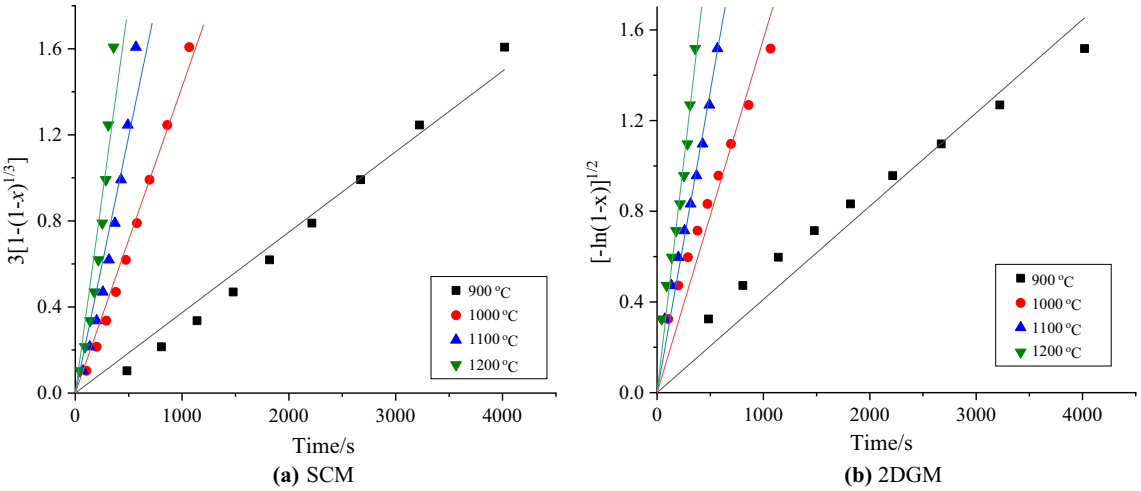

Fig. 6 Plots of linearized SCM and 2DGM for WS char gasification

Table 6 Reaction constants (k) of high-alkali chars based on the SCM and 2DGM

Temperature/°C	WS char		LA char		ZJ char		TC char	
	k_{SCM}	k_{2DGM}	k_{SCM}	k_{2DGM}	k_{SCM}	k_{2DGM}	k_{SCM}	k_{2DGM}
900	0.00037	0.00041	0.00016	0.00018	0.00029	0.00032	0.00033	0.00037
1000	0.00142	0.00156	0.00080	0.00089	0.00088	0.00099	0.00087	0.00098
1100	0.00239	0.00266	0.00139	0.00157	0.00126	0.00142	0.00126	0.00142
1200	0.00363	0.00406	0.00182	0.00204	0.00133	0.00150	0.00145	0.00163

the external reactant is consumed, so the core of unreacted char continues to shrink during the conversion process [51, 52]. The 2DGM is a kind of Avrami and Erofe'ev model ($m = 2$), which assumes that "germ nuclei" of the new phase are distributed randomly inside the char particle and then the new phase grows throughout the char particle until the conversion is finished [39, 43]. The different accuracies of SCM and 2DGM at different reaction temperatures indicate that most of CO_2 reacts with carbon at the outside surface of WS char particle at low temperature (900 °C and 1000 °C), while more CO_2 moves into the char particle and react with the inside carbon at relatively high temperature (1100 °C and 1200 °C). In the cases of the three chars originated from the high-alkali coals, it is apparent that the 2DGM is remarkably more precise to describe the gasification behavior than the SCM at 900–1200 °C. Approximately, the SCM overpredicts the gasification at $x < 0.7$ and underpredicts it at $x > 0.7$, while the 2DGM predicts the opposite. Even so, the calculated $x \sim t$ curves based on the 2DGM are closer to the experimental data and the averaged *MAPE*s for LA, ZJ, and TC chars based on the 2DGM (12.6%, 10.6%, and 8.4%, respectively) are significantly smaller than those based on the SCM (28.0%, 32.1%, and 33.7%, respectively). It implies that CO_2 tends to seep into the pores of char particle and react with the inside carbon instead of being consumed at the external particle surface.

The 2DGM ($m = 2$) rather than the SCM ($m = 1.07$) is more appropriate to study the char gasification in most cases according to Fig. 7, though the values of m in Table 4 are not very close to 2. It is possibly due to the range of conversion ratio. Usually, x was limited to the acceleratory region ($x = 0.15$–0.50), which was considered to be qualified for exploring reaction mechanisms [39, 42, 43]. However, the previous research mainly focused on the reactions of simple substances, such as the transformation of β-$CuAlCl_4$ to α-$CuAlCl_4$ [42], the reduction of hematite to wustite [43], and the decomposition of some salts [39]. When it comes to complex char gasification, some researchers employed the kinetic method with different x range to obtain m. Wang et al. [41] extended the range of carbon conversion ratio ($x = 0.15$–0.60) to conduct the kinetic analysis of pinewood gasification. They also calculated the values of m when $x = 0.60$–0.98 to select a better kinetic model. In addition, Sharp and Hancock, who developed this method of kinetic analysis, pointed out that a wider range of x was acceptable if it was difficult to select a kinetic model that perfectly matches the

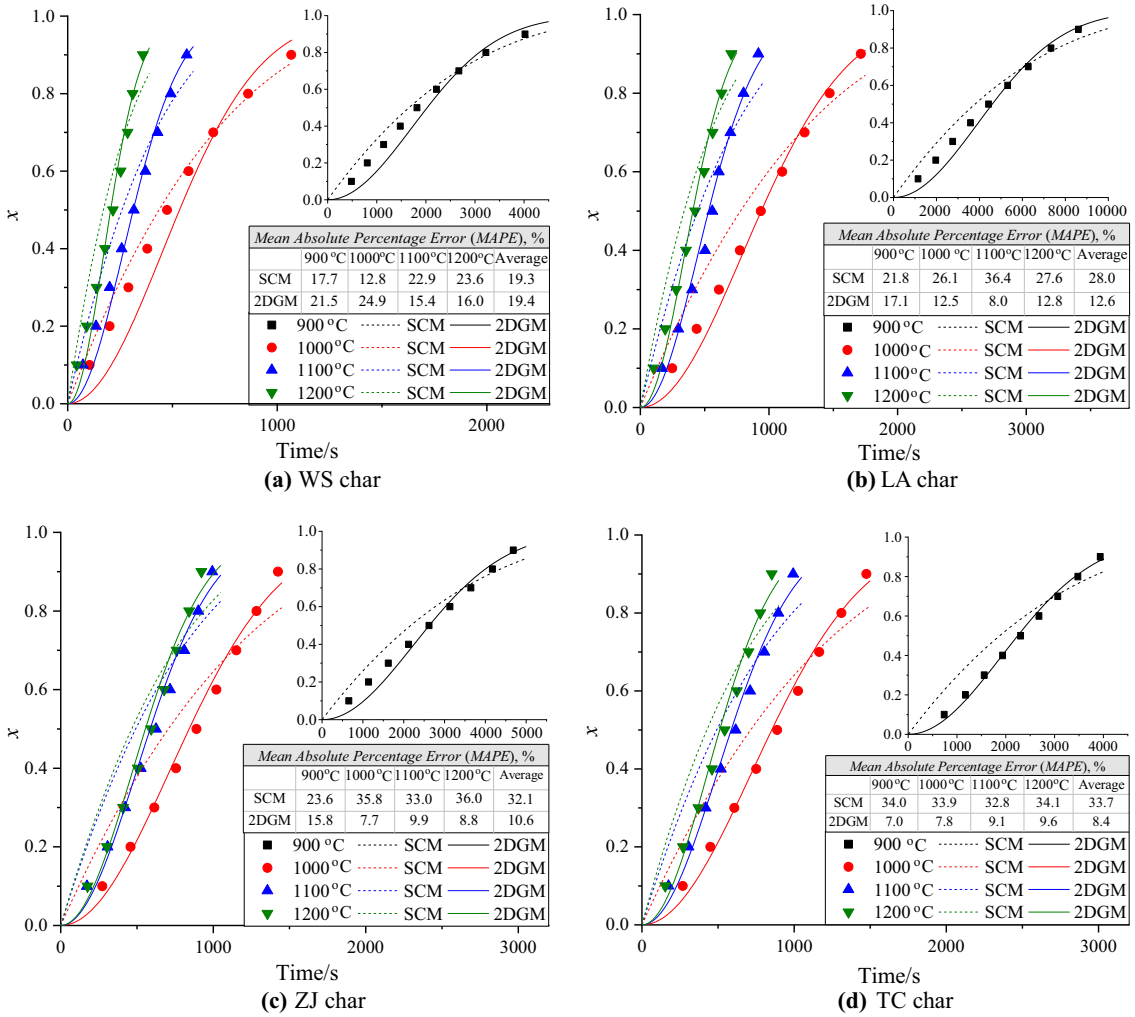

Fig. 7 Comparison of experimental data and calculated curves of high-alkali chars based on the SCM and 2DGM

Table 7 Fitting parameters of high-alkali chars in the wider range of x

Temperature/°C	WS char		LA char		ZJ char		TC char	
	m (x=0.15–0.70)	m (x=0.15–0.90)	m (x=0.15–0.70)	m (x=0.15–0.90)	m (x=0.15–0.70)	m (x=0.15–0.90)	m (x=0.15–0.70)	m (x=0.15–0.90)
900	1.41	1.44	1.43	1.49	1.42	1.51	1.71	1.80
1000	1.33	1.33	1.53	1.58	1.75	1.82	1.71	1.77
1100	1.39	1.47	1.82	1.83	1.65	1.71	1.66	1.73
1200	1.38	1.41	1.51	1.56	1.71	1.81	1.66	1.74

original m [39]. According to the experimental data, wider x range leads to bigger m. Table 7 lists the fitting parameters in the range of x = 0.15–0.70 and x = 0.15–0.90. As listed in Tables 4 and 7, the values of m in the range of x = 0.15–0.70 are clearly closer to 2 than the corresponding ones in Table 4 (x = 0.15–0.50), and the values of m in the range of x = 0.15–0.90 are even bigger. Consequently, the superiority of the 2DGM (m = 2) over the SCM (m = 1.07) makes more sense if the x range is extended properly in the present study.

Table 8 Fitting parameters of SC char with or without chemicals in the range of $x = 0.15–0.70$

Temperature/°C	SC char		SC char + Na_2SO_4		SC char + $CaCO_3$		SC char + Fe_2O_3	
	m	R^2	m	R^2	m	R^2	m	R^2
900	1.07	0.9824	1.39	0.9948	0.92	0.9990	1.11	0.9982
1000	1.64	0.9726	1.46	0.9916	1.54	0.9976	1.20	0.9961
1100	1.71	0.9615	1.60	0.9919	1.57	0.9927	1.37	0.9868
1200	1.73	0.9602	1.61	0.9853	1.60	0.9903	1.71	0.9908

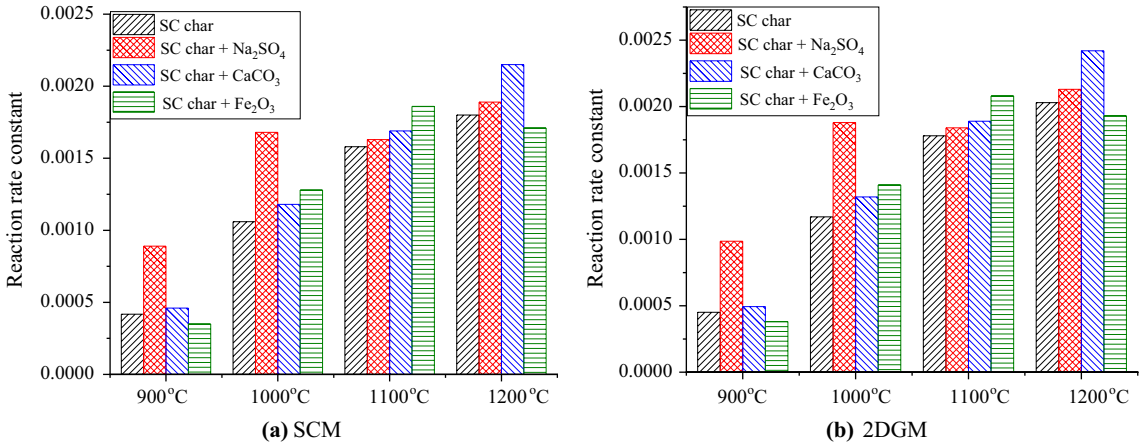

Fig. 8 Reaction constants (k) of SC char with or without chemicals based on the SCM and 2DGM

Kinetic analysis of gasification catalyzed by minerals related to high-alkali fuels

Three common related to the high-alkali fuels, Na_2SO_4, $CaCO_3$, and Fe_2O_3, were selected to further study the effects of minerals on high-alkali char gasification through the kinetic analysis. According to the Avrami and Erofe'ev equations (Eqs. 3 and 4), the fitting parameters were calculated in the range of $x = 0.15–0.70$ and listed in Table 8. Since most values of m fluctuates between 1 and 2, the SCM and 2DGM have also been employed. Based on the two models, the reaction constants (k) of SC char with or without chemicals were determined by linear regression analysis, and the results are depicted in Fig. 8. As shown, the addition of Na_2SO_4 increases greatly the reaction constants at 900 °C and 1000 °C, while the promoting impacts are weak at 1100 °C and 1200 °C. The reaction constants of SC char with $CaCO_3$ are higher than those of SC char without chemicals, especially at 1200 °C. Though Fe_2O_3 enhances the char gasification at 1000 °C and 1100 °C, this chemicals decreases the reaction constants at 900 °C and 1200 °C. Both the 2DGM and SCM indicate that the influences of those chemicals are temperature-dependent.

In order to evaluate the effects of those chemicals on the accuracies of selected kinetic models, the calculated $x \sim t$ curves based on the SCM and 2DGM are compared with the experiment data in Fig. 9. The SCM is more precise to describe the gasification behavior of SC char at 900 °C, and the addition of $CaCO_3$ or Fe_2O_3 affects insignificantly the accuracy of SCM. However, the calculated $x \sim t$ curve based on the 2DGM is closer to the experiment data when Na_2SO_4 is added into the SC char at 900 °C. It seems that Na_2SO_4 tends to change the reaction mechanism from the SCM to 2DGM. According to the ash compositions in Table 2, Na_2SO_4 is supposed to be commonly present in the three high-alkali coal chars, while WS char, as a biomass char, contains no Na. Perhaps it is one of the reasons that the 2DGM rather than the SCM is more suitable for the three high-alkali coal chars at 900 °C, which is opposite for WS char (as shown in Fig. 7). The 2DGM is more qualified than the SCM to predict the conversion of SC char with Na_2SO_4 and $CaCO_3$ at 1000 °C. However, the SCM is more accurate for the gasification of SC char catalyzed by Fe_2O_3. Although the Fe does not usually exist as the oxide in raw fuel, Fe_2O_3 is often identified in the ash samples of some high-alkali fuels [19]. Hence, the effect of Fe_2O_3 on the reaction mechanism should be taken into account if the high-alkali fuel ash and some other additives containing Fe_2O_3 serve as catalysts. At 1100 °C and 1200 °C, the 2DGM is more accurate to describe the gasification behavior of SC char, whether there are Na_2SO_4, $CaCO_3$, and Fe_2O_3, or not.

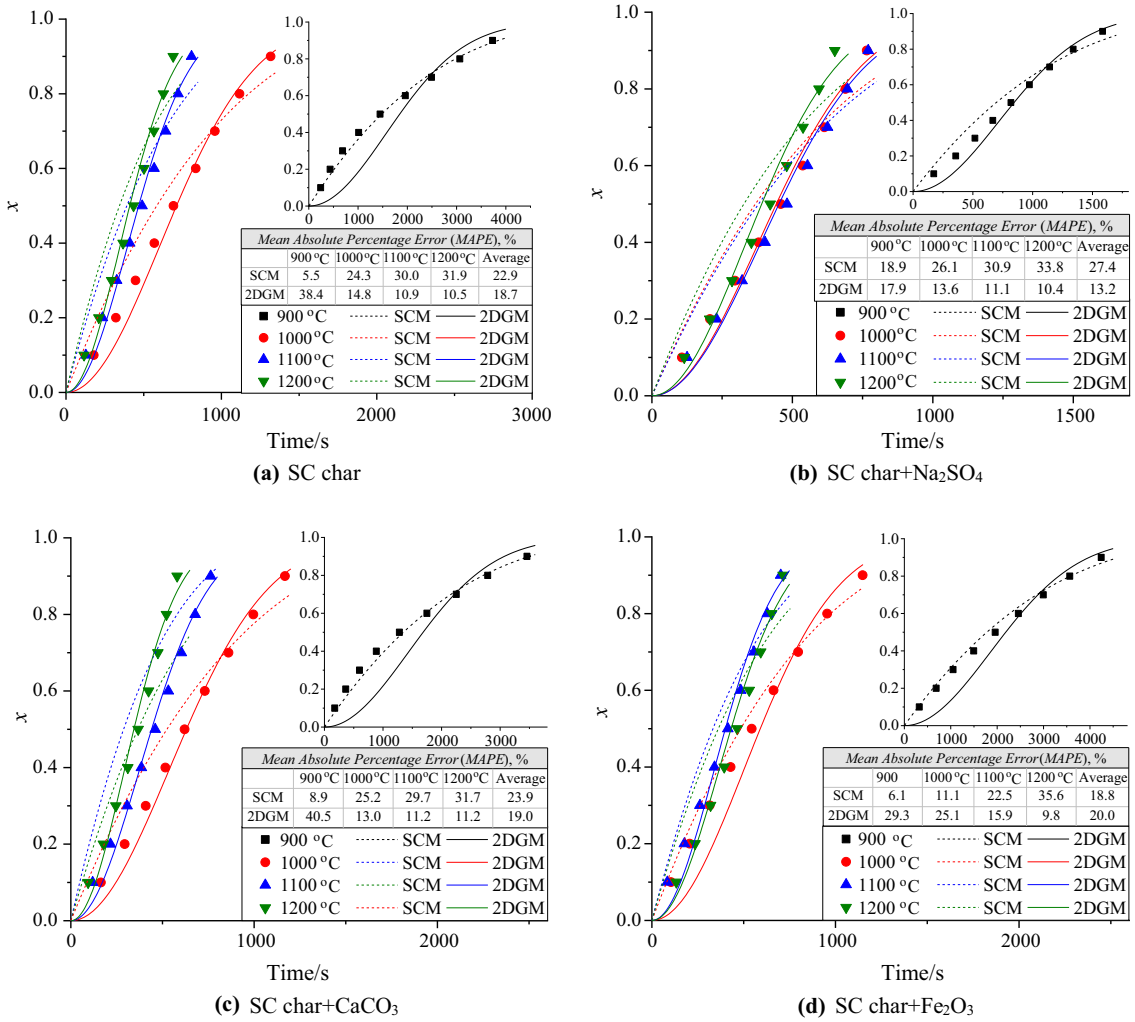

Fig. 9 Comparison of experimental data and calculated curves of SC char with or without chemicals based on the SCM and 2DGM

Conclusions

In this paper, experimental and kinetic study on the CO_2 gasification behavior of chars originated from one high-alkali biomass (WS) and three high-alkali coals (LA, ZJ, and TC coals) was carried out. The effects of minerals related to high-alkali fuels (Na, K, Ca, and Fe species) were also evaluated via synthetic coal char. The shrinking core model (SCM) and two-dimensional growth of nuclei model (2DGM) were selected to conduct the kinetic analysis. The results indicate that the gasification reactivities of chars from high-alkali fuels are positively associated with the reaction temperature. The WS char possesses the highest gasification reactivity, and three coal char samples are inferior to various degrees. The widespread minerals on the surfaces of WS char are supposed to be one of the reasons. The gasification behavior of synthetic coal (SC) char is similar to those of real char, which means SC char is qualified to study the impacts of minerals related to high-alkali fuels. The related minerals, which are determined through the new plasma ashing method and traditional muffle ashing method, mostly can enhance the char gasification at 1000 °C. Generally, these chemicals offer their catalytic activities at 1000 °C in the sequence of K/Na-containing chemicals > Fe-containing chemicals > Ca-containing chemicals.

The reaction constants of chars from different high-alkali fuels are consistent with their gasification behavior. The SCM is more suitable to predict the gasification behavior of WS char at 900 °C and 1000 °C, while the 2DGM is better at 1100 °C and 1200 °C. It implies that for WS char, CO_2 is mostly consumed at the external particle surface at low temperature, while it tends to seep into the pores of char particle and react with the inside carbon at high temperature. When it comes to the three high-alkali coal chars, the 2DGM is remarkably more precise than SCM at 900–1200 °C. In most cases, the additions of

chemicals increase the reaction constants. When Fe_2O_3 and $CaCO_3$ are added into SC char, the SCM is still more accurate to describe the gasification behavior at 900 °C, but the addition of Na_2SO_4 makes the 2DGM a better one.

Acknowledgements The authors acknowledge the financial support from the National Natural Science Foundation of China (No. 52176129).

Authors' contribution Conceptualization: LZ, CW; Data curation: LZ; Formal analysis: LZ; Funding acquisition: CW, DC; Investigation: LZ, ML, PZ; Methodology: LZ; Project administration: CW, DC; Resources: CW, DC; Software: LZ; Supervision: CW; Validation: CW; Visualization: LZ; Writing—Original Draft: LZ; Writing—Review and Editing: CW.

References

1. Niu YQ, Tan HZ, Hui SE. Ash-related issues during biomass combustion: alkali-induced slagging, silicate melt-induced slagging (ash fusion), agglomeration, corrosion, ash utilization, and related countermeasures. Prog Energy Combust Sci. 2016;52:1–61.
2. Demirbas A. Combustion characteristics of different biomass fuels. Prog Energy Combust Sci. 2004;30(2):219–30.
3. Zhang S, Chen C, Shi D, Lü J, Wang J, Guo X, et al. Situation of combustion utilization of high sodium coal. Proc CSEE. 2013;33:1–12.
4. Safarian S, Unnþórsson R, Richter C. A review of biomass gasification modelling. Renew Sustain Energy Rev. 2019;110:378–91.
5. Toftegaard MB, Brix J, Jensen PA, Glarborg P, Jensen AD. Oxy-fuel combustion of solid fuels. Prog Energy Combust Sci. 2010;36(5):581–625.
6. Sun LT, Sun R, Yan YH, Yuan MF, Wu JQ. Investigation of air-MILD and oxy-MILD combustion characteristics of semicoke and bituminous coal mixtures in a 0.3 MW fuel-rich/lean fired furnace. Fuel Process Technol. 2022;231:107247.
7. Puig-Arnavat M, Bruno JC, Coronas A. Review and analysis of biomass gasification models. Renew Sustain Energy Rev. 2010;14(9):2841–51.
8. Xiang YL, Cai L, Guan YW, Liu WB, Cheng ZY, Liu ZX. Study on the effect of gasification agents on the integrated system of biomass gasification combined cycle and oxy-fuel combustion. Energy. 2020;206: 118131.
9. Chen DG, Zhang Z, Li ZS, Lv Z, Cai NS. Optimizing in-situ char gasification kinetics in reduction zone of pulverized coal air-staged combustion. Combust Flame. 2018;194:52–71.
10. Ding L, Dai ZH, Wei JT, Zhou ZJ, Yu GS. Catalytic effects of alkali carbonates on coal char gasification. J Energy Inst. 2017;90(4):588–601.
11. Mei YG, Wang ZQ, Fang YT, Huang JJ, Li WZ, Guo S, et al. CO_2 catalytic gasification with $NaAlO_2$ addition for its low-volatility and tolerant to deactivate. Fuel. 2019;242:160–6.
12. Ohtsuka Y, Tomita A. Calcium catalysed steam gasification of Yallourn brown coal. Fuel. 1986;65(12):1653–7.
13. Lahijani P, Zainal ZA, Mohamed AR, Mohammadi M. CO_2 gasification reactivity of biomass char: catalytic influence of alkali, alkaline earth and transition metal salts. Bioresour Technol. 2013;144:288–95.
14. Zhang JB, Jiang PP, Gao FL, Ren ZY, Li R, Chen HY, et al. Fuel gas production and char upgrading by catalytic CO_2 gasification of pine sawdust char. Fuel. 2020;280: 118686.
15. Zhang F, Xu DP, Wang YG, Argyle MD, Fan MH. CO_2 gasification of Powder River Basin coal catalyzed by a cost-effective and environmentally friendly iron catalyst. Appl Energy. 2015;145:295–305.
16. Wang CA, Zhu X, Liu X, Lv Q, Zhao L, Che DF. Correlations of chemical properties of high-alkali solid fuels: a comparative study between Zhundong coal and biomass. Fuel. 2018;211:629–37.
17. Guo S, Jiang YF, Liu T, Zhao JT, Huang JJ, Fang YT. Investigations on interactions between sodium species and coal char by thermogravimetric analysis. Fuel. 2018;214:561–8.
18. Wang YW, Wang ZQ, Huang JJ, Fang YT. Investigation into the characteristics of Na_2CO_3-catalyzed steam gasification for a high-aluminum coal char. J Therm Anal Calorim. 2018;131(2):1213–20.
19. Wang CA, Zhao L, Liu CC, Gao XY, Li GY, Che DF. Comparative study on ash characteristics of various high-alkali fuels using different ashing methods and temperatures. Fuel. 2021;299: 120912.
20. Qin YH, He YY, Ren WP, Gao MJ, Wiltowski T. Catalytic effect of alkali metal in biomass ash on the gasification of coal char in CO_2. J Therm Anal Calorim. 2020;139(5):3079–89.
21. Mukherjee S, Srivastava SK. Minerals transformations in north-eastern region coals of India on heat treatment. Energy Fuels. 2006;20(3):1089–96.
22. Wang CA, Zhao L, Yuan MB, Liu CC, Wang CW, Zhao L, et al. Effects of ashing method and blending on ash characteristics of pyrolyzed and gasified semi-cokes. Fuel. 2020;271: 117607.
23. Wang CA, Zhao L, Yuan MB, Du YB, Zhu CZ, Liu YH, et al. Effects of minerals containing sodium, calcium, and iron on oxy-fuel combustion reactivity and kinetics of Zhundong coal via synthetic coal. J Therm Anal Calorim. 2020;139(1):261–71.
24. Wang CA, Du YB, Che DF. Reactivities of coals and synthetic model coal under oxy-fuel conditions. Thermochim Acta. 2013;553:8–15.
25. Xu J, Yang Y, Li YW. Recent development in converting coal to clean fuels in China. Fuel. 2015;152:122–30.
26. Kok MV. Simultaneous thermogravimetry–calorimetry study on the combustion of coal samples: Effect of heating rate. Energy Convers Manag. 2012;53(1):40–4.
27. Kok MV, Topa E. Thermal characterization and model-free kinetics of biodiesel sample. J Therm Anal Calorim. 2015;122(2):955–61.
28. Xin HH, Wang HT, Kang WJ, Di CC, Qi XY, Zhong XX, et al. The reburning thermal characteristics of residual structure of lignite pyrolysis. Fuel. 2020;259: 116226.
29. Zhao RD, Qin JG, Chen TJ, Wang LL, Wu JH. Experimental study on co-combustion of low rank coal semicoke and oil sludge by TG-FTIR. Waste Manag. 2020;116:91–9.
30. Yadav D, Saha S, Sahu G, Chavan PD, Datta S, Chauhan V, et al. A comparative review on thermal behavior of feedstocks during gasification via thermogravimetric analyzer. J Therm Anal Calorim. 2023;148(2):329–54.
31. Wang CA, Feng QQ, Mao QS, Wang CW, Li GY, Che DF. Oxy-fuel co-combustion performances and kinetics of bituminous coal and ultra-low volatile carbon-based fuels. Int J Energy Res. 2021;45(2):1892–907.
32. Zuo HB, Geng WW, Zhang JL, Wang GW. Comparison of kinetic models for isothermal CO_2 gasification of coal char-biomass char blended char. Int J Miner, Metall, Mater. 2015;22(4):363–70.
33. He Q, Guo QH, Ding L, Wei JT, Yu GS. CO_2 gasification of char from raw and torrefied biomass: Reactivity, kinetics and mechanism analysis. Bioresour Technol. 2019;293: 122087.
34. Saha S, Sahu G, Chavan PD, Datta S. Gasification reactivity of high ash Indian coals in varying concentrations of CO_2. Int J Oil, Gas Coal Technol. 2018;18(1–2):163–86.
35. Li L, Wang ZQ, Zhao R, Mei YG, Shi WJ, Liu ZY, et al. The different catalytic effects of Na species on char gasification and the reasons for this different. J Therm Anal Calorim. 2022;147(10):5687–99.

36. Yan XY, Hu JJ, Zhang QG, Zhao SH, Dang JT, Wang W. Chemical-looping gasification of corn straw with Fe-based oxygen carrier: thermogravimetric analysis. Bioresour Technol. 2020;303:122904.
37. Fermoso J, Gil MV, Pevida C, Pis JJ, Rubiera F. Kinetic models comparison for non-isothermal steam gasification of coal–biomass blend chars. Chem Eng J. 2010;161(1):276–84.
38. Wang GW, Zhang JL, Hou XM, Shao JG, Geng WW. Study on CO_2 gasification properties and kinetics of biomass chars and anthracite char. Bioresour Technol. 2015;177:66–73.
39. Hancock J, Sharp J. Method of comparing solid-state kinetic data and its application to the decomposition of kaolinite, brucite, and $BaCO_3$. J Am Ceram Soc. 2006;55:74–7.
40. Hu Q, Yang HP, Xu HS, Wu ZQ, Lim CJ, Bi XT, et al. Thermal behavior and reaction kinetics analysis of pyrolysis and subsequent in-situ gasification of torrefied biomass pellets. Energy Convers Manag. 2018;161:205–14.
41. Wang T, Tang LF, Raheem A, Chen XL, Wang FC. Study on CO_2 gasification characteristics of pyrolysis char from pinewood block and pellet. Biomass Convers Biorefin 2021.
42. Liu HM, Sullivan RM, Hanson JC, Grey CP, Martin JD. Kinetics and mechanism of the β- to α-$CuAlCl_4$ phase transition: A time-resolved ^{63}Cu MAS NMR and powder X-ray diffraction study. J Am Chem Soc. 2001;123(31):7564–73.
43. Piotrowski K, Mondal K, Wiltowski T, Dydo P, Rizeg G. Topochemical approach of kinetics of the reduction of hematite to wüstite. Chem Eng J. 2007;131(1):73–82.
44. Betancur M, Natalia Arenas C, Daniel Martínez J, Victoria Navarro M, Murillo R. CO_2 gasification of char derived from waste tire pyrolysis: kinetic models comparison. Fuel. 2020;273:117745.
45. Kumari N, Saha S, Sahu G, Chauhan V, Roy R, Datta S, et al. Comparison of CO_2 gasification reactivity and kinetics: petcoke, biomass and high ash coal. Biomass Convers Biorefin. 2022;12(6):2277–90.
46. Wang G, Zhang J, Hou X, Shao J, Geng W. Study on CO_2 gasification properties and kinetics of biomass chars and anthracite char. Biores Technol. 2015;177:66–73.
47. Mathews JP, Krishnamoorthy V, Louw E, Tchapda AHN, Castro-Marcano F, Karri V, et al. A review of the correlations of coal properties with elemental composition. Fuel Process Technol. 2014;121:104–13.
48. Krishnamoorthy V, Pisupati SV. A critical review of mineral matter related issues during gasification of coal in fixed, fluidized, and entrained flow gasifiers. Energies. 2015;8(9):10430–63.
49. Li C, Wang Y, Lin X, Tian Z, Wu X, Yang Y, et al. Influence of inherent minerals on CO_2 gasification of a lignite with high ash content. J Fuel Chem Technol. 2017;45(7):780–8.
50. Lü L, Li C, Zhang GQ, Hu XW, Liang B. Decomposition behavior of $CaSO_4$ during potassium extraction from a potash feldspar-$CaSO_4$ binary system by calcination. Chin J Chem Eng. 2018;26(4):838–44.
51. Szekely J, Evans JW. A structural model for gas-solid reactions with a moving boundary. Chem Eng Sci. 1970;25(6):1091–107.
52. Adamon DGF, Fagbémi LA, Bensakhria A, Sanya EA. Comparison of kinetic models for carbon dioxide and steam gasification of rice husk char. Waste Biomass Valoriz. 2019;10(2):407–15.